

## Electrochemically Controlled Formation/Dissociation of Phosphonate-Cavitand/Methylpyridinium Complexes

Benoît Gadenne,<sup>[a]</sup> Monica Semeraro,<sup>[a]</sup> Roger M. Yebeutchou,<sup>[b]</sup> Francesca Tancini,<sup>[b]</sup> Laura Pirondini,<sup>[b]</sup> Enrico Dalcanale,<sup>\*[b]</sup> and Alberto Credi<sup>\*[a]</sup>

**Abstract:** The phosphorus-bridged cavitand **1** self-assembles very efficiently in CH<sub>2</sub>Cl<sub>2</sub> with either the monopyridinium guest **2**<sup>+</sup> or the bispyridinium guest **3**<sup>2+</sup>. In the first case a 1:1 complex is obtained, whereas in the second case both 1:1 and 2:1 host-guest complexes are observed. The association between **1** and either one of the guests causes the quenching of the cavitand fluorescence; in the case of the adduct between **1** and **3**<sup>2+</sup>, the fluorescence of

the latter is also quenched. Cavitand complexation is found to affect the reduction potential values of the electroactive guests. Voltammetric and spectroelectrochemical measurements show that upon one-electron reduction both guests are released from the cavity of

**1.** Owing to the chemical reversibility of such redox processes, the supramolecular complexes can be re-assembled upon removal of the extra electron from the guest. Systems of this kind are promising for the construction of switchable nanoscale devices and self-assembling supramolecular materials, the structure and properties of which can be reversibly controlled by electrochemical stimuli.

**Keywords:** cavitands • electrochemistry • host-guest systems • luminescence • supramolecular chemistry

### Introduction

In recent years cavitand chemistry has expanded from the usual host-guest topics into the emerging fields of molecular devices, sensors and materials, as documented by the following examples. Supramolecular sensors for the selective detection of aromatic VOC in air at sub-ppb level have been proposed with cavitands as the recognition unit.<sup>[1]</sup> Chemically controlled nanoscale tweezers have been obtained by harnessing the reversible switching between a contracted (vase) and an expanded (kite) conformation of cavitands derivatised with two rigid arms.<sup>[2]</sup> Cavitand-based capsules that

host linear alkenes by constraining them into high-energy conformations could be employed to make spring-loaded nanomachines.<sup>[3]</sup> Highly adaptive oligomeric materials, operating in multimodal fashion through the implementation of two orthogonal self-assembling interactions, namely solvophobic aggregation and metal coordination, have been generated starting from a specifically designed cavitand precursor.<sup>[4]</sup>

Apart from these pioneering examples, the possibility of using made-to-order cavitands as components of dynamic molecular devices and materials<sup>[5]</sup> is still relatively unexplored. In particular, the ability of cavitands to form complexes with guests that can be switched chemically, photochemically or electrochemically<sup>[6]</sup> would allow the development of supramolecular systems, the structure and properties of which could be modulated by external stimulation.<sup>[7,8]</sup>

Phosphonate cavitands<sup>[9]</sup> occupy a unique position within the large cavitand family,<sup>[10]</sup> owing to their versatile complexation properties. Tetrakisphosphonate cavitands in their all inward configuration<sup>[11]</sup> are able to complex positively charged species, such as ammonium salts or inorganic cations, with very high association constants ( $K_{\text{ass}} = 10^7 - 10^9 \text{ M}^{-1}$ ).<sup>[12]</sup> They also bind selectively, but reversibly, C<sub>1</sub>-C<sub>4</sub> linear alcohols at the gas-solid interface.<sup>[13]</sup>

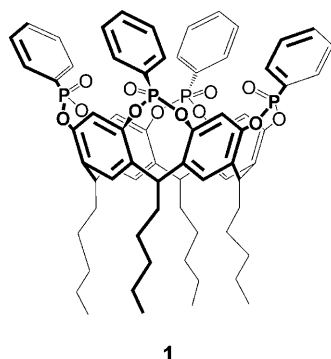
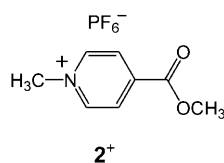
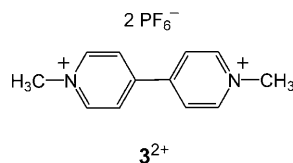
In this study we have employed photophysical and electrochemical techniques to probe the interaction between the

[a] Dr. B. Gadenne, Dipl.-Chem. M. Semeraro, Prof. A. Credi  
Dipartimento di Chimica "G. Ciamician"  
Università di Bologna, Via Selmi 2, 40126 Bologna (Italy)  
Fax: (+39)051-209-9456  
E-mail: alberto.credi@unibo.it

[b] Dr. R. M. Yebeutchou, Dipl.-Chem. F. Tancini, Dr. L. Pirondini,  
Prof. E. Dalcanale  
Dipartimento di Chimica Organica e Industriale and INSTM  
UdR Parma, Università di Parma  
Viale Usberti 17 A, 43100 Parma (Italy)  
Fax: (+39)0521-905472  
E-mail: enrico.dalcanale@unipr.it

Supporting information for this article is available on the WWW under <http://dx.doi.org/10.1002/chem.200800966>.

phosphorus-bridged cavitand **1**,<sup>[9]</sup> and two pyridinium-type guests, namely 4-carbomethoxy-1-methylpyridinium (**2**<sup>+</sup>) and 1,1'-dimethyl-4,4'-bipyridinium (methyl viologen; **3**<sup>2+</sup>) in solution. Specifically, we have investigated the absorption, luminescence and voltammetric properties of the resulting supramolecular complexes, determined their association constants, and assessed the effect of electrochemical reduction of the guest on their stability. The structures of the examined compounds are depicted here; the positively charged guests were used as their hexafluorophosphate salts.

**1****2**<sup>+</sup>**3**<sup>2+</sup>

## Results and Discussion

**Absorption and luminescence properties:** The absorption and luminescence data for the examined compounds at room temperature are gathered in Table 1 and shown in Figure 1. The cavitand **1** exhibits a moderately intense and structured absorption band in the near UV region ( $\lambda_{\max} = 272$  nm), and a structureless fluorescence emission with  $\lambda_{\max} = 303$  nm. The monopyridinium guest **2**<sup>+</sup> shows an absorption band with  $\lambda_{\max} = 274$  nm, and no emission. The bispyridinium guest **3**<sup>2+</sup> (methyl viologen) is very poorly soluble in  $\text{CH}_2\text{Cl}_2$ ; therefore its photophysical data are reported

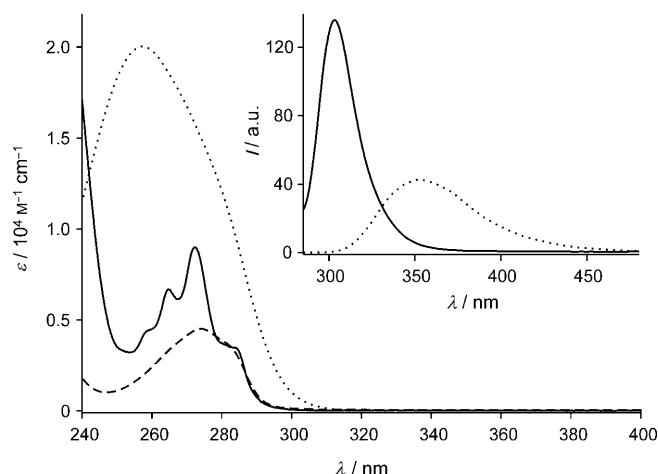


Figure 1. Absorption and fluorescence (inset) spectra of cavitand **1** (—), and guests **2**<sup>+</sup> (---) and **3**<sup>2+</sup> (.....) in  $\text{CH}_2\text{Cl}_2$  at room temperature. For the fluorescence spectra, excitation was performed at the corresponding absorption maximum.

in MeCN. Methyl viologen exhibits an intense absorption band with  $\lambda_{\max} = 260$  nm, and a structureless fluorescence band with  $\lambda_{\max} = 353$  nm.

**Complex of **1** and **2**<sup>+</sup>:** The absorption spectrum of a 1:1 mixture of **1** and **2**<sup>+</sup> is slightly different from the sum of the absorption spectra of the isolated species (see Supporting Information). Specifically, the appearance of an absorption tail in the 280–310 nm region suggests the occurrence of electronic interactions between **1** and **2**<sup>+</sup>.

Titration of the cavitand with **2**<sup>+</sup> leads to absorption spectral changes that are dominated by the absorbance increase due to addition of the guest. Instead, the fluorescence band of **1** is strongly quenched upon addition of **2**<sup>+</sup> (Figure 2). The titration curve points to the formation of an adduct with 1:1 stoichiometry and apparent  $\log K = 6.6 \pm 0.1$ . This value is consistent with the one obtained from isothermal titration calorimetry (ITC) measurements ( $\log K = 6.89 \pm 0.03$ ).<sup>[14]</sup> The driving force for complex formation is mainly provided by cation–dipole interactions between the N<sup>+</sup> atom of the guest and the P=O moieties of **1** pointing towards the interior of the cavity.<sup>[12,14,15]</sup> It can be noted that a fluorescence emission, corresponding to about 10% of the initial intensity, is still observed at the end of the titration. A careful comparison with the band shape of the fluorescence of free **1** shows that the emission band of the cavitand in the presence of an excess of **2**<sup>+</sup> has a more pronounced low-energy tail (see Supporting Information). Such a residual emission shows a double exponential decay with  $\tau_1 = 2.7$  ns

Table 1. Photophysical and electrochemical data for the examined compounds at room temperature.

	Spectroscopic data					Electrochemical data <sup>[b]</sup>	
	Absorption <sup>[a]</sup>		Luminescence <sup>[a]</sup>			$E'/V$ vs. SCE <sup>[c]</sup>	$E''/V$ vs. SCE <sup>[c]</sup>
	$\lambda_{\max}$ [nm]	$\epsilon$ [ $\text{M}^{-1} \text{cm}^{-1}$ ]	$\lambda_{\max}$ [nm]	$\tau$ [ns]	$\Phi$		
<b>1</b>	272	9000	303	2.5	0.06	[d]	[d]
<b>2</b> <sup>+</sup>	274	4500	[e]	[e]	[e]	−0.65	−1.52 <sup>[f]</sup>
<b>3</b> <sup>2+</sup>	260 <sup>[g]</sup>	20 000 <sup>[g]</sup>	353 <sup>[g]</sup>	0.9 <sup>[g]</sup>	0.02 <sup>[g]</sup>	−0.21 <sup>[h]</sup>	−0.77 <sup>[h]</sup>

[a] Air equilibrated solution in  $\text{CH}_2\text{Cl}_2$ . [b] Electrochemical data for the different compounds ( $10^{-3}$  M) in  $\text{CH}_2\text{Cl}_2$ , 0.1 M tetrabutylammonium hexafluorophosphate as supporting electrolyte, glassy carbon electrode; ferrocene was used as an internal reference,  $E_{\text{Fc}^+/\text{Fc}} = +0.51$  V vs. SCE. [c] Halfwave potential values of mono-electronic and chemically reversible processes, unless otherwise noted. [d] Not electroactive. [e] Not luminescent. [f] Chemically irreversible process; potential value of the DPV peak at a scan rate of  $20 \text{ mV s}^{-1}$ . [g] Air equilibrated solution in  $\text{CH}_3\text{CN}$ . [h] Data referred to 1,1'-dioctyl-4,4'-bipyridinium because of the very low solubility of **3**<sup>2+</sup> in  $\text{CH}_2\text{Cl}_2$ .

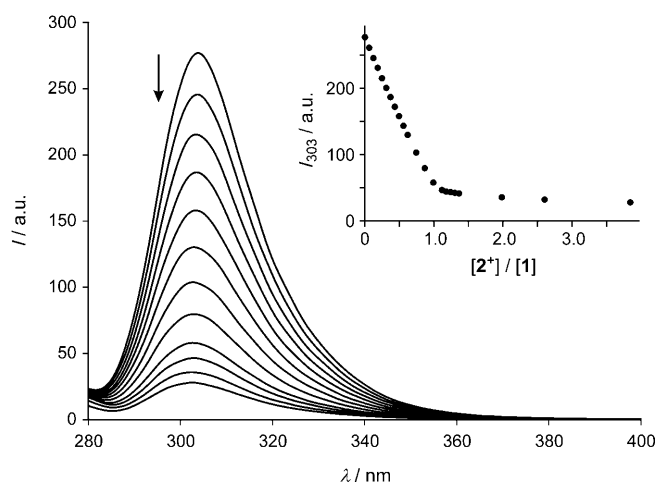


Figure 2. Fluorescence changes ( $\lambda_{\text{exc}}=272$  nm) upon titration of **1** ( $1.56 \times 10^{-3}$  M) with  $2^+$  in  $\text{CH}_2\text{Cl}_2$  at room temperature (curves refer to 0, 0.12, 0.25, 0.37, 0.50, 0.62, 0.74, 0.87, 0.99, 1.24, 1.98 and 3.84 equiv of  $2^+$ ). The inset shows the titration curve obtained by monitoring the fluorescence intensity of **1** at 303 nm.

and  $\tau_2 < 1$  ns. The longer component is responsible for 90% of the emitted intensity and is assigned to uncomplexed cavitant species ( $\tau=2.5$  ns, Table 1), whereas the shorter component is assigned to emission from the  $[\mathbf{1}\cdot\mathbf{2}]^+$  complex, which, as noted above, exhibits a slightly different luminescence band relative to free **1**.

It should be noted that a non-negligible residual amount of free cavitant species is present even for saturating concentrations of the guest (Figure 2, inset). This observation can be explained by assuming that the self-assembly of the complex is in competition with the formation of tight ion pairs between the positively charged guests and their counterions. As a matter of fact, it was often observed<sup>[16–19]</sup> that in apolar solvents the association between a positively charged guest  $G^+$  and an uncharged host H [Eq. (1)] is hampered by ion pairing of the former species [Eq. (2)], unless the guest ion pairs are maintained upon complexation, or specific stabilisation of the guest counterions ( $A^-$ ) can be provided by the host itself.<sup>[20,21]</sup>



In the titration experiment, the result of which is depicted in Figure 2, the guest is added as a  $\text{PF}_6^-$  salt. Therefore, as the concentration of  $2^+$  and  $\text{PF}_6^-$  ions increases throughout the titration, the formation of ion pairs becomes increasingly more likely. Apparently, the fraction of the guest that is ion-paired is not available for complexation by **1**, a corresponding fraction of which remains thus free in solution and can be revealed by luminescence spectroscopy. Supporting evidence for the effect of the counterions on complex formation arises from the fact that the addition of a large excess of tetrabutylammonium hexafluorophosphate (TBAPF<sub>6</sub>) to

a solution containing **1** and  $2^+$  in a 1:2 ratio causes an increase of the luminescence band with  $\lambda_{\text{max}}=303$  nm. Taken together, these findings suggest that 1) the complex is not ion-paired and 2) the addition of anions causes its disassembly. The crystal structure of a related *N*-methylpyridinium complex supports this view, since in the solid state the  $\text{PF}_6^-$  counterion is located outside the cavity.<sup>[15]</sup> This issue is further discussed in the next sections.

**Complexes of 1 and  $3^{2+}$ :** Addition of small aliquots of a concentrated solution of  $3^{2+}$  in MeCN to a solution of **1** in  $\text{CH}_2\text{Cl}_2$  causes changes in the absorption and luminescence spectra (Figure 3) that are consistent with the formation of

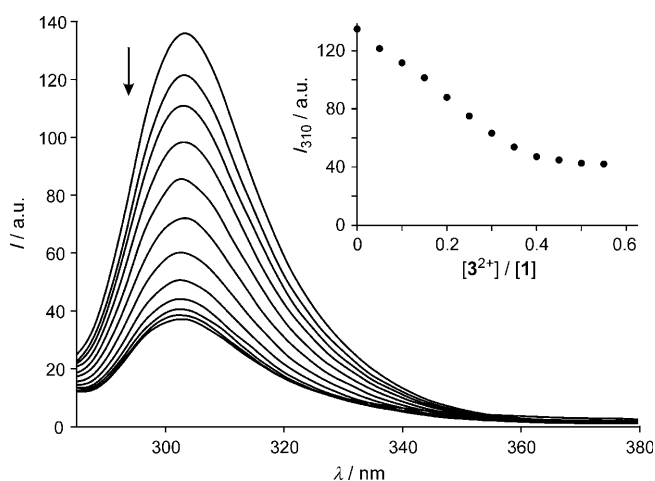


Figure 3. Fluorescence spectral changes ( $\lambda_{\text{exc}}=271$  nm) observed upon titration of a  $7.8 \times 10^{-6}$  M solution of **1** in  $\text{CH}_2\text{Cl}_2$  with small aliquots of a concentrated solution of  $3^{2+}$  in MeCN (curves refer to 0, 0.05, 0.10, 0.20, 0.30, 0.35, 0.40, 0.45, 0.50 and 0.55 equiv of  $3^{2+}$ ). The inset shows the titration curve obtained by monitoring the fluorescence intensity of **1** at 310 nm.

an adduct between these components. Specifically, both the fluorescence of **1** and  $3^{2+}$  are quenched when the components are mixed. The decrease of fluorescence of the free cavitant stops after addition of 0.5 equiv of  $3^{2+}$  (Figure 3, inset); concomitantly, the fluorescence of free  $3^{2+}$  is not observed until after the addition of more than 0.5 equivalents of guest (see Supporting Information). All these observations point to the formation of a 2:1 adduct in which two cavitands encapsulate one methyl viologen species (for the crystal structure of a related 2:1 methyl viologen/cavitant adduct see reference [12]).

Also in this case a residual luminescence signal at 310 nm is observed for saturating concentrations of the guest (Figure 3). This emission exhibits a monoexponential decay with  $\tau=2.4$  ns and therefore has to be attributed to the free cavitant. The addition of a large excess of TBAPF<sub>6</sub> to a solution containing **1** and  $3^{2+}$  in  $\text{CH}_2\text{Cl}_2$  in a 1:2 ratio causes an increase of the luminescence band of the host. As discussed in the case of the complexation of  $2^+$  by **1**, these observations can be explained by considering that the interac-

tion between the cavitands and  $3^{2+}$  is hampered by the formation of ion pairs between the latter species and its  $\text{PF}_6^-$  counterions.<sup>[16–19]</sup>

The reverse titration, namely, the addition of cavitand to a solution of  $3^{2+}$ , leads to interesting results. First of all, the absorption spectrum of a very dilute ( $1.2 \times 10^{-5} \text{ M}$ ) solution of  $3^{2+}$  in  $\text{CH}_2\text{Cl}_2$  shows a band in the near UV region that is much broader than that observed in MeCN, with a tail towards the red region reaching down to 400 nm (Figure 4).

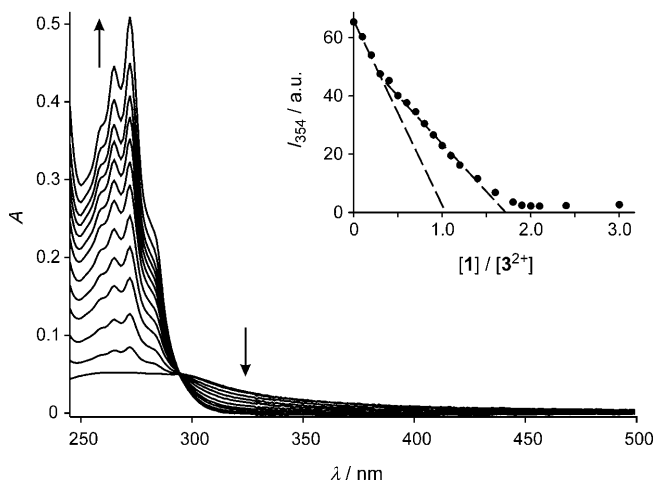


Figure 4. Absorption spectral changes observed upon titration of  $3^{2+}$  ( $1.2 \times 10^{-5} \text{ M}$ ) with **1** in  $\text{CH}_2\text{Cl}_2$  at room temperature (curves refer to 0, 0.20, 0.40, 0.60, 0.80, 1.00, 1.20, 1.40, 1.60, 1.80, 2.00, 2.40 and 3.00 equiv of **1**). The inset shows the fluorescence titration curve obtained from the emission intensity of  $3^{2+}$  at 354 nm upon excitation at 300 nm. Dashed lines represent a guide to the eye (not a fitting) for the two different slopes of the titration plot.

This behaviour is most likely related to aggregation phenomena involving the poorly soluble  $3^{2+}$  species. Addition of **1** causes the progressive disappearance of this absorption tail and the quenching of the luminescence band of  $3^{2+}$  (Figure 4). The luminescence characteristic of free **1** does not show up until more than two equivalents of **1** have been added. The fluorescence titration plot (Figure 4, inset) is consistent with the formation of two adducts, with 1:1 and 2:1 (host/guest) stoichiometries. Clearly, complexation by **1** prevents the formation of aggregates of  $3^{2+}$  species in  $\text{CH}_2\text{Cl}_2$ . The stepwise stability constants for the 1:1 and the 2:1 complexation are  $\log K_1 = 6.3 \pm 0.1$  and  $\log K_2 = 6.3 \pm 0.3$ , respectively. Such observations show that 1) the affinity of methyl viologen for the cavity of **1** is similar to that of the *N*-methylpyridinium guest  $2^+$  and 2) complexation of methyl viologen by the first cavitand does not hamper the association of a second cavitand molecule. Taken together, these results suggest that a molecule of **1** can interact independently with either one of the *N*-methylpyridinium ends of  $3^{2+}$ .

A qualitative extrapolation of the two different slopes of the titration plot (dashed lines in Figure 4, inset) shows that the quenching of the methyl viologen luminescence is very

strong both in the 1:1 and in the 2:1 adducts. The value of the quenching rate constant, calculated from Equation (3) in which  $\tau_0$  and  $I_0$  are the luminescence lifetime and intensity of  $3^{2+}$  in the absence of **1**, and  $I$  is the luminescence intensity of  $3^{2+}$  in the presence of an excess of **1**, exceeds  $5 \times 10^{10} \text{ s}^{-1}$ . Interestingly, the lack of any residual methyl viologen luminescence after titration of a dilute solution of its hexafluorophosphate salt with **1** shows that the ion pairing between  $3^{2+}$  and  $\text{PF}_6^-$  is not important in these conditions, in agreement with the fact that the amount of anions remains constant and small throughout the experiment.

$$k_q = 1/\tau_0(I_0/I - 1) \quad (3)$$

The titration of  $3^{2+}$  by **1** was also performed in  $\text{CH}_2\text{Cl}_2/\text{MeCN}$  8:2 (*v/v*) in order to afford good solubility of methyl viologen and avoid its intermolecular aggregation. Under these conditions, the absorption spectrum of  $3^{2+}$  is almost identical to that observed in MeCN, thereby showing no aggregation. The changes in the luminescence bands of **1** and  $3^{2+}$  are qualitatively similar to those observed in pure  $\text{CH}_2\text{Cl}_2$  and are consistent with the formation of 1:1 and 2:1 adducts, albeit with slightly lower apparent stability constants ( $\log K_1 = 6.00 \pm 0.04$  and  $\log K_2 = 5.6 \pm 0.1$ , respectively). The presence of 20% MeCN reduces the strength of complexation, indicating that guest solvation plays a significant role in the process, together with cation–dipole interactions between the charged guest and the four P=O groups, and CH– $\pi$  interactions of the *N*-Me group of the guest with the cavity.<sup>[15]</sup>

Because the electrochemical experiments are performed in the presence of tetrabutylammonium hexafluorophosphate as supporting electrolyte and the spectroscopic experiments evidenced a counterion effect on the stability of the complexes, we decided to investigate the association of **1** and  $3^{2+}$  in  $\text{CH}_2\text{Cl}_2$  in the presence of 0.1 M TBAPF<sub>6</sub>. As expected, the presence of such an electrolyte lowers the apparent stability constant for both the 1:1 and 2:1 adducts ( $\log K_1 = 5.16 \pm 0.03$  and  $\log K_2 = 3.9 \pm 0.7$ , respectively). However, these values still ensure that, in a 2:1 mixture of **1** and  $3^{2+}$  in the conditions of the voltammetric and spectroelectrochemical experiments, more than 90% of the species are associated to give the  $[(\mathbf{1})_2 \cdot \mathbf{3}]^{2+}$  complex.

**Electrochemical properties:** The electrochemical data for the examined compounds in  $\text{CH}_2\text{Cl}_2/\text{TBAPF}_6$  at room temperature are gathered in Table 1. The cavitand is not electroactive in the potential window examined (from  $-1.8 \text{ V}$  to  $+1.8 \text{ V}$  vs. SCE). The 4-carbomethoxy-1-methylpyridinium guest  $2^+$  shows two reduction processes and no oxidation. The first reduction process is chemically reversible and mono-electronic ( $E'_{1/2} = -0.65 \text{ V}$ , Figure 5a); the second one also involves the exchange of one electron and is poorly reversible ( $E''_p = -1.52 \text{ V}$ ; potential of the DPV peak at a scan rate of  $20 \text{ mVs}^{-1}$ ). Since methyl viologen is not soluble enough in  $\text{CH}_2\text{Cl}_2$  in order to perform voltammetric experiments, 1,1'-dioctyl-4,4'-bipyridinium (dioctyl viologen) was

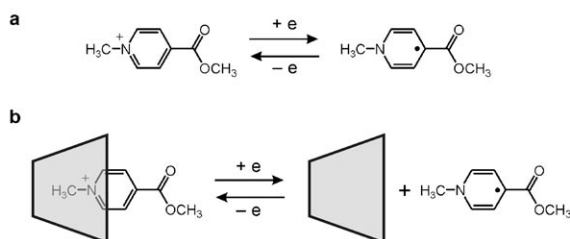
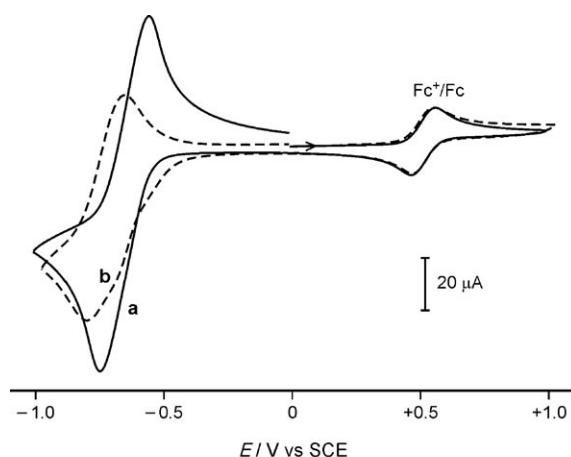


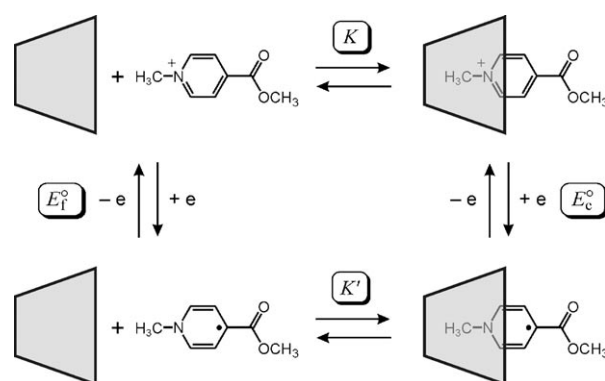
Figure 5. Cyclic voltammograms for the first reduction of  $2^+$  alone (a, —) and in the presence of one equivalent of **1** (b, ---). The reversible wave at +0.51 V is that of ferrocene, used as a standard. The bottom schemes represent the processes corresponding to each voltammogram curve (see text for details). Conditions:  $1.2 \times 10^{-3}$  M,  $\text{CH}_2\text{Cl}_2/\text{TBAPF}_6$ ,  $200 \text{ mV s}^{-1}$ , glassy carbon electrode.

employed as a model<sup>[22]</sup> for the electroactive bipyridinium unit of  $3^{2+}$ . On the other hand, dioctyl viologen cannot be used as a guest for **1**, because the two octyl chains can neither be accommodated in the inner space of the cavitand nor pierce its lower rim. Dioctyl viologen shows<sup>[21,22]</sup> two reversible monoelectronic reduction processes with  $E'_{1/2} = -0.21 \text{ V}$  and  $E''_{1/2} = -0.77 \text{ V}$  vs. SCE (see Figure 7a).

**Complex of 1 and  $2^+$ :** The addition of one equivalent of **1** to a solution of  $2^+$  in  $\text{CH}_2\text{Cl}_2$  causes a shift of the first reduction process of the guest to more negative potentials, and a decrease of the corresponding current intensity (Figure 5). These observations are in agreement with the fact that  $2^+$  forms a complex with the cavitand, and can be interpreted on the basis of the square pattern shown in Scheme 1, in which two complexation equilibria (horizontal reactions) are coupled with two redox processes (vertical reactions).<sup>[23]</sup> The two association constants,  $K$  and  $K'$ , are related to the standard potential values of the free and complexed  $2^+$  ( $E_t^0$  and  $E_c^0$ , Scheme 1) by Equation (4):<sup>[23]</sup>

$$\frac{K}{K'} = \exp\left[\frac{F}{RT}(E_t^0 - E_c^0)\right] \quad (4)$$

On the basis of Equation (4), taking the halfwave potential values for reduction of  $2^+$  alone ( $-0.65 \text{ V}$  vs. SCE,



Scheme 1. Square scheme representing the coupling of the redox processes of the guest  $2^+$  (vertical processes) with the complexation equilibria with cavitand **1** (horizontal processes).

Table 1) and in the presence of one equivalent of **1** ( $-0.75 \text{ V}$  vs. SCE, Figure 5) as  $E_t^0$  and as the upper limit of  $E_c^0$ , respectively,<sup>[24]</sup> one can estimate that  $K'$  is at least 50 times smaller than  $K$ . Therefore, one-electron reduction of the guest leads to a substantial decrease in the stability of the complex. The fact that the second reduction process is not affected by the presence of **1** (see Supporting Information) is in full agreement with this interpretation, and indicates that in our conditions the monoelectronic reduction of the guest leads to disassembly of the complex.<sup>[25]</sup> This behaviour can be accounted for by considering that one-electron reduction of  $2^+$  affords a neutral species with no affinity for the host and enhanced solvation in  $\text{CH}_2\text{Cl}_2$ . The electron-acceptor character of the guest is strongly diminished upon reduction, thereby suppressing the cation–dipole interactions between the charged guest and the converging P=O units. On subsequent reoxidation of the reduced guest  $2^\bullet$  the complex is re-assembled, as shown by the reversibility of the wave shown in Figure 5b.

To gain more insight on whether one-electron reduction of the guest leads to complex disassembly, we have performed spectroelectrochemical experiments. The absorption spectrum of the monoreduced  $2^\bullet$  species (Figure 6), obtained upon electrolysis of  $2^+$  at  $-1.1 \text{ V}$  versus an Ag pseudo-reference electrode, shows two intense bands with  $\lambda_{\text{max}} = 304$  and  $395 \text{ nm}$ . The shape of the absorption bands arising from reduction of the  $2^+$  guest in the  $[\mathbf{1}\cdot\mathbf{2}]^+$  complex (Figure 6) is identical to that of the absorption bands obtained for free  $2^\bullet$  species. Therefore, the spectroelectrochemical results support the conclusion that the complex is disassembled upon one-electron reduction of the guest.

**Complexes of 1 and  $3^{2+}$ :** In the presence of two equivalents of **1**, the methyl viologen guest  $3^{2+}$  can be dissolved in  $\text{CH}_2\text{Cl}_2$  to a concentration sufficient for voltammetric experiments. Under these conditions, the first reduction process of  $3^{2+}$  is considerably shifted to more negative potentials compared to the same process in the dioctyl viologen model compound (Figure 7). This observation is in agreement with the fact that  $3^{2+}$  forms a stable 2:1 (host/guest)

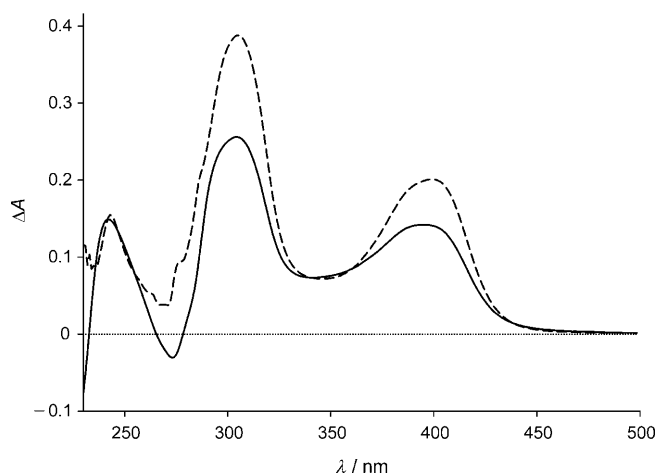


Figure 6. Difference absorption spectra obtained upon electrochemical reduction of **2**<sup>+</sup> alone (—) and in the presence of one equivalent of **1** (---) at  $-1.1$  V versus an Ag pseudo-reference electrode in a spectroelectrochemical thin-layer cell ( $2.3 \times 10^{-3}$  M,  $\text{CH}_2\text{Cl}_2/\text{TBAPF}_6$ ).

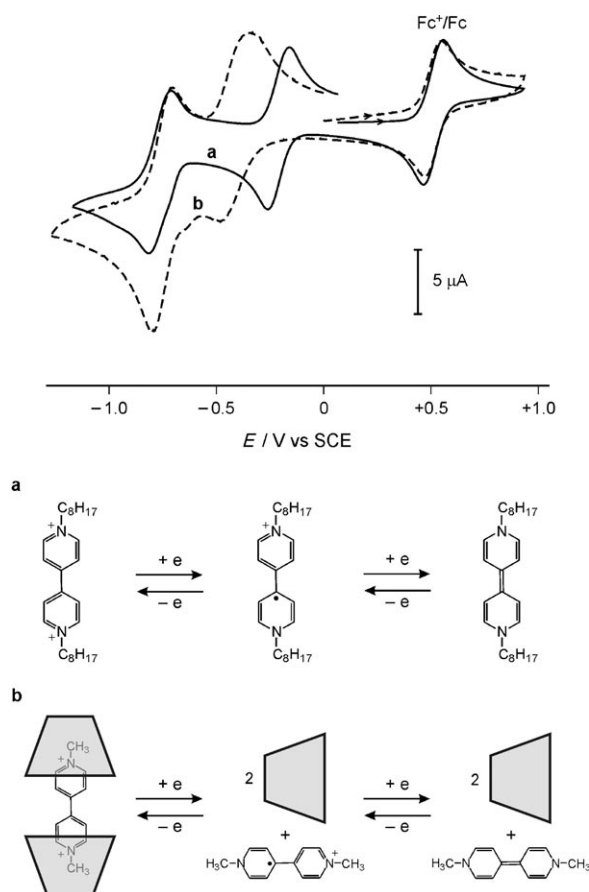


Figure 7. Cyclic voltammograms for reduction of dioctyl viologen alone (a, —) and of **3**<sup>2+</sup> in the presence of two equivalents of **1** (b, ---). The reversible wave at  $+0.51$  V is that of ferrocene, used as a standard. The bottom schemes represent the processes corresponding to each voltammogram curve (see text for details). Conditions:  $1.05 \times 10^{-3}$  M,  $\text{CH}_2\text{Cl}_2/\text{TBAPF}_6$ ,  $200 \text{ mV s}^{-1}$ , glassy carbon electrode.

complex with the cavitand, and can be interpreted on the basis of considerations similar to those discussed for the **2**<sup>+</sup> guest. The second reduction process takes place at the same potential observed for the corresponding process in dioctyl viologen (Figure 7), suggesting that one-electron reduction of the guest leads to disassembly of the complex for the same reasons taken into account in the case of the previous system. It is known<sup>[26]</sup> that the added electron in **3**<sup>2+</sup> is extensively delocalised, thereby equally diminishing the positive charge of both nitrogen atoms and, as a consequence, weakening the cation–dipole interactions with both cavitand hosts. The reversibility of the first reduction wave shown in Figure 7b indicates that on subsequent reoxidation of the monoreduced guest **3**<sup>2+</sup> the complex is re-assembled.

The above hypothesis is supported by the results of spectroelectrochemical measurements. The absorption spectrum of the monoreduced **3**<sup>2+</sup> species (Figure 8), obtained upon electrolysis of **3**<sup>2+</sup> at  $-0.5$  V versus an Ag pseudo-reference electrode, shows the typical<sup>[22]</sup> absorption spectrum of the bipyridinium radical cation, with two intense and structured bands peaking at  $\lambda_{\text{max}} = 400$  and  $605$  nm. The absorption spectrum obtained upon reduction of the  $[(\mathbf{1})_2\mathbf{3}]^{2+}$  complex in the same conditions is nearly identical to that of free monoreduced dioctyl viologen (Figure 8). If the monoreduced guest remained included in **1**, it would be expected that the absorption spectrum of the former would be affected in some way<sup>[27,28]</sup> relative to that recorded in the absence of the cavitand. Therefore, the spectroelectrochemical results are in agreement with the dissociation of the  $[(\mathbf{1})_2\mathbf{3}]^{2+}$  complex upon one-electron reduction of the guest.

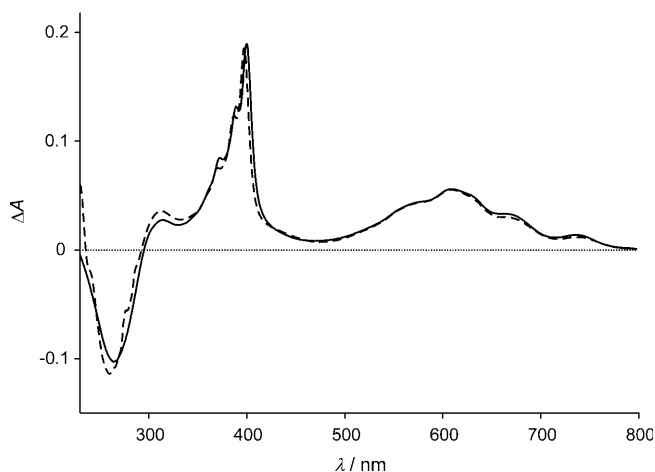


Figure 8. Difference absorption spectra obtained upon electrochemical reduction of dioctyl viologen alone (—) and of **3**<sup>2+</sup> in the presence of two equivalents of **1** (---) at  $-0.5$  V versus an Ag pseudo-reference electrode in a spectroelectrochemical thin-layer cell ( $5.5 \times 10^{-4}$  M,  $\text{CH}_2\text{Cl}_2/\text{TBAPF}_6$ ).

## Conclusion

Cavitand **1** forms stable complexes with mono- and bispyridinium guests in dichloromethane. The complexes have 1:1



stoichiometry in the case of the monopyridinium guest, whereas the bispyridinium guest is complexed by two cavitand molecules. Formation of the complexes substantially affects the photophysical and electrochemical properties of the molecular components. Specifically, the observed luminescence of the free host and guest species is strongly quenched when they are associated. Luminescence experiments allowed us to determine the  $K$  values of the complexes formed under different conditions. Increasing the solvent polarity and the ionic strength of the medium leads to a reduction of the complexes stability, as quantified in the case of  $[(\mathbf{1})_2\cdot\mathbf{3}]^{2+}$  complex.

Electrochemical experiments show that one-electron reduction of the guests leads to decomplexation. Since the mono-electronic reduction of the investigated guests is reversible, the formation and dissociation of such complexes can be electrochemically controlled. These results are of interest because they constitute a first step towards the development of supramolecular devices and materials, for example, supramolecular polymers,<sup>[15,29]</sup> that can be electrochemically assembled and disassembled. Research in this direction is underway in our laboratories.

## Experimental Section

**Synthesis of 1:** *N*-Methylpyrrolidine (0.151 mL, 1.46 mmol) and dichlorophenylphosphine oxide (0.649 mL, 4.57 mmol) were added to a solution of pentyl-footed resorcinarene<sup>[30]</sup> (0.80 g, 1.04 mmol) in distilled toluene (30 mL) at room temperature. The resultant mixture was heated to reflux and vigorously stirred for 5 h. The reaction mixture was cooled to room temperature and concentrated in vacuo. Aluminium oxide column chromatography ( $\text{CH}_2\text{Cl}_2/\text{MeOH}$  98:2) of the crude afforded the **1** stereoisomer as a white powder (0.58 g, 0.46 mmol, 46%).  $^1\text{H}$  NMR (300 MHz, 298 K,  $\text{CDCl}_3$ ):  $\delta$  = 8.00 (m, 8H; P(O)ArH<sub>o</sub>), 7.66–7.49 (m, 4H+8H+4H; P(O)ArH<sub>p</sub> + P(O)ArH<sub>m</sub> + ArH<sub>down</sub>), 6.90 (s, 4H; ArH<sub>up</sub>), 4.75 (m, 4H; ArCH), 2.49 (m, 8H;  $\text{CH}_2(\text{CH}_2)_3\text{CH}_3$ ), 1.53–1.30 (m, 24H;  $\text{CH}_2(\text{CH}_2)_3\text{CH}_3$ ), 0.89 ppm (t,  $J$  = 7.0 Hz, 12H;  $\text{CH}_2(\text{CH}_2)_3\text{CH}_3$ );  $^{31}\text{P}$  NMR (162 MHz, 298 K,  $\text{CDCl}_3$ ):  $\delta$  = 7.63 ppm (s, P=O); ESI-MS:  $m/z$  calcd for  $\text{C}_{72}\text{H}_{76}\text{O}_{12}\text{P}_4$  (1257.3 Da)  $[\text{M}+\text{Na}]^+$ : 1280.3; found 1280;  $[\text{M}+\text{K}]^+$ : 1296.4; found 1296.

**Absorption and luminescence experiments:** Measurements were carried out at room temperature (ca. 295 K) on air-equilibrated solutions of the samples in  $\text{CH}_2\text{Cl}_2$  (Merck Uvasol) or  $\text{CH}_3\text{CN}$  (Merck Uvasol) in the concentration range from  $1 \times 10^{-6}$  to  $2 \times 10^{-5}$  M. UV/Vis absorption spectra were recorded with a Perkin–Elmer  $\lambda$ 40 spectrophotometer. Luminescence spectra were obtained with an LS-50 spectrofluorimeter (Perkin–Elmer) equipped with a Hamamatsu R928 phototube. Correction of the luminescence intensity for inner filter effects was performed when necessary according to a previously reported procedure.<sup>[31]</sup> Luminescence lifetimes were measured by the time-correlated single-photon counting (TCSPC) technique with Edinburgh Instruments FLS920 equipment. The spectrophotometric and spectrofluorimetric titration curves were analysed with the SPECFIT software.<sup>[32]</sup> The experimental error on molar absorption coefficients, emission intensities, and luminescence lifetimes is estimated to be  $\pm 5\%$ , on wavelength values,  $\pm 1$  nm. The quenching rate constant of the luminescence of  $\mathbf{3}^{2+}$  in its complexes with **1** was estimated from Equation (3) (see main text).

**Electrochemical experiments:** Cyclic voltammetric (CV) and differential pulse voltammetric (DPV) experiments were carried out in argon-purged  $\text{CH}_2\text{Cl}_2$  (Romil Hi-Dry) at room temperature with an Autolab 30 multi-purpose instrument interfaced to a PC. The working electrode was a glassy carbon electrode (Amel;  $0.07 \text{ cm}^2$ ), the counter electrode was a Pt

wire, separated from the solution by a frit, and an Ag wire was employed as a quasi-reference electrode. Ferrocene was present as an internal standard ( $E_{1/2} = +0.51 \text{ V}$  vs. SCE). The concentration of the compounds examined was on the order of  $1 \times 10^{-3}$  M; tetrabutylammonium hexafluorophosphate 0.1 M was added as supporting electrolyte. Under these conditions, the observed potential window ranged from  $-1.8$  to  $+1.8 \text{ V}$  vs. SCE. CVs were obtained at sweep rates varying from 0.02 to  $2 \text{ V s}^{-1}$ . DPVs were obtained at a sweep rate of  $0.02 \text{ mV s}^{-1}$ , with a pulse height of 75 mV and a duration of 40 ms. The IR compensation implemented within the Autolab 30 was used, and every effort was made throughout the experiments to minimise the resistance of the solution. In any instance, the full electrochemical reversibility of the voltammetric wave of ferrocene was taken as an indicator of the absence of uncompensated resistance effects. For reversible processes the halfwave potential values were calculated from an average of CV and DPV experiments, whereas the redox potential values in the case of irreversible processes were estimated from the DPV peaks. Experimental errors: potential values,  $\pm 10 \text{ mV}$  for reversible processes,  $\pm 20 \text{ mV}$  for irreversible processes. Spectroelectrochemical measurements were performed in situ with a custom-made optically transparent thin-layer electrochemical (OTTLE) cell by using an Autolab 30 potentiostat and an Agilent Technologies 8543 diode array spectrophotometer. The working and counter electrodes were Pt minigrids, and the quasi-reference electrode was an Ag wire; all the electrodes were melt-sealed into a polyethylene spacer. The thickness of the layer, determined by spectrophotometry, was about  $180 \mu\text{m}$ . The curves reported in Figures 6 and 8 show the difference between the absorption spectra of the solution after and before the electrolysis.

## Acknowledgements

Financial support from the EU (STREP “Biomach” and NoE “MAG-MANet”), Ministero dell’Università e della Ricerca (PRIN 2006034123 003), and Regione Emilia-Romagna (NANOFABER) is gratefully acknowledged.

- [1] S. Zampolli, P. Betti, I. Elmi, E. Dalcanale, *Chem. Commun.* **2007**, 2790–2792.
- [2] a) V. A. Azov, A. Schlegel, F. Diederich, *Bull. Chem. Soc. Jpn.* **2006**, 79, 1926–1940; b) V. A. Azov, A. Beeby, M. Cacciarini, A. G. Cheetham, F. Diederich, M. Frei, J. K. Gimzewski, V. Gramlich, B. Hecht, B. Jaun, T. Latychevskaia, A. Lieb, Y. Lill, F. Marotti, A. Schlegel, R. R. Schlitter, P. J. Skinner, P. Seiler, Y. Yamakoshi, *Adv. Funct. Mater.* **2006**, 16, 147–156; c) V. A. Azov, A. Schlegel, F. Diederich, *Angew. Chem.* **2005**, 117, 4711–4715; *Angew. Chem. Int. Ed.* **2005**, 44, 4635–4638; d) M. Frei, F. Diederich, R. Tremont, T. Rodriguez, L. Echegoyen, *Helv. Chim. Acta* **2006**, 89, 2040–2057.
- [3] a) J. Rebek, Jr., *Chem. Commun.* **2007**, 2777–2789; b) D. Ajami, J. Rebek, Jr., *J. Am. Chem. Soc.* **2006**, 128, 15038–15039; c) M. P. Schramm, J. Rebek, Jr., *Chem. Eur. J.* **2006**, 12, 5924–5933.
- [4] L. Pirondini, A. G. Stendardo, S. Geremia, M. Campagnolo, P. Samorì, J. P. Rabe, R. Fokkens, E. Dalcanale, *Angew. Chem.* **2003**, 115, 1422–1425; *Angew. Chem. Int. Ed.* **2003**, 42, 1384–1387.
- [5] J.-M. Lehn, *Chem. Soc. Rev.* **2007**, 36, 151–170.
- [6] *Molecular Switches*, 2nd ed. (Ed.: B. L. Feringa), Wiley-VCH, Weinheim, **2008**.
- [7] V. Balzani, A. Credi, M. Venturi, *Molecular Devices and Machines—Concepts and Perspectives for the Nanoworld*, Wiley-VCH, Weinheim, **2008**.
- [8] Recent examples: a) Y. H. Ling, J. T. Mague, A. E. Kaifer, *Chem. Eur. J.* **2007**, 13, 7908–7914; b) B. J. Jordan, M. A. Pollier, L. A. Miller, C. Tiernan, G. Clavier, P. Audebert, V. M. Rotello, *Org. Lett.* **2007**, 9, 2835–2838; c) S. Silvi, A. Arduini, A. Pochini, A. Secchi, M. Tomasulo, F. M. Raymo, M. Baroncini, A. Credi, *J. Am. Chem. Soc.* **2007**, 129, 13378–13379; d) S. Angelos, Y. W. Yang, K. Patel, J. F. Stoddart, J. I. Zink, *Angew. Chem.* **2008**, 120, 2254–2258; *Angew.*

- Chem. Int. Ed.* **2008**, *47*, 2222–2226; e) H. Tian, L. Feng, *J. Mater. Chem.* **2008**, *18*, 1617–1622; f) K. Yamauchi, Y. Takashima, A. Hashidzume, H. Yamaguchi, A. Harada, *J. Am. Chem. Soc.* **2008**, *130*, 5024–5025.
- [9] For a review on phosphonate cavitands and the nomenclature adopted see: R. Pinalli, M. Suman, E. Dalcanale, *Eur. J. Org. Chem.* **2004**, 451–462.
- [10] D. J. Cram, J. M. Cram, *Container Molecules and Their Guests*, The Royal Society of Chemistry, Cambridge, **1994**.
- [11] P. Delangle, J.-P. Dutasta, *Tetrahedron Lett.* **1995**, *36*, 9325–9328.
- [12] J.-P. Dutasta, *Top. Curr. Chem.* **2004**, *232*, 55–91.
- [13] M. Melegari, M. Suman, L. Pirondini, D. Moiani, C. Massera, F. Uguzzoli, E. Kalenius, P. Vainiotalo, J.-C. Mulatier, J.-P. Dutasta, E. Dalcanale, *Chem. Eur. J.* **2008**, *14*, 5772–5779.
- [14] E. Biavardi, G. Battistini, M. Montalti, R. M. Yebeutchou, L. Prodi, E. Dalcanale, *Chem. Commun.* **2008**, 1638–1640.
- [15] R. M. Yebeutchou, F. Tancini, N. Demitri, S. Geremia, R. Mendichi, E. Dalcanale, *Angew. Chem.* **2008**, *120*, 4580–4584; *Angew. Chem. Int. Ed.* **2008**, *47*, 4504–4508.
- [16] M. Montalti, L. Prodi, *Chem. Commun.* **1998**, 1461–1462.
- [17] J. W. Jones, H. W. Gibson, *J. Am. Chem. Soc.* **2003**, *125*, 7001–7004.
- [18] F. Huang, J. W. Jones, C. Slebodnik, H. W. Gibson, *J. Am. Chem. Soc.* **2003**, *125*, 14458–14464.
- [19] M. Clemente-León, C. Pasquini, V. Hebbe-Viton, J. Lacour, A. Dalla Cort, A. Credi, *Eur. J. Org. Chem.* **2006**, 105–112.
- [20] For reviews on ion-pair recognition, see: a) M. T. Reetz, in *Comprehensive Supramolecular Chemistry*, Vol. 2 (Eds.: J. L. Atwood, J. E. D. Davies, D. D. Macnicol, F. Vögtle, J.-M. Lehn), Pergamon Press, Oxford, **1996**, p. 553; b) P. A. Gale, *Coord. Chem. Rev.* **2003**, *240*, 191–221; c) P. A. Gale, S. E. Garcia-Garrido, J. Garric, *Chem. Soc. Rev.* **2008**, *37*, 151–190.
- [21] A. Credi, S. Dumas, S. Silvi, M. Venturi, A. Arduini, A. Pochini, A. Secchi, *J. Org. Chem.* **2004**, *69*, 5881–5887.
- [22] R. Ballardini, A. Credi, M. T. Gandolfi, C. Giansante, G. Marconi, S. Silvi, M. Venturi, *Inorg. Chim. Acta* **2007**, *360*, 1072–1082.
- [23] A. E. Kaifer, M. Gómez-Kaifer, *Supramolecular Electrochemistry*, Wiley-VCH, Weinheim, **1999**, Chapter 9.
- [24] As the reduced and oxidised forms of the species considered here should exhibit very similar diffusion coefficients, we can safely assume that the standard potentials are coincident with the halfwave potentials.
- [25] For examples of redox-controlled assembly-disassembly of host-guest complexes, see references [8a,b,g], [21] and: a) G. Cooke, *Angew. Chem.* **2003**, *115*, 5008–5018; *Angew. Chem. Int. Ed.* **2003**, *42*, 4860–4870; b) W. S. Jeon, E. Kim, Y. H. Ko, I. H. Hwang, J. W. Lee, S. Y. Kim, H. J. Kim, K. Kim, *Angew. Chem.* **2005**, *117*, 89–93; *Angew. Chem. Int. Ed.* **2005**, *44*, 87–91; c) W. Wang, A. E. Kaifer, *Angew. Chem.* **2006**, *118*, 7200–7204; *Angew. Chem. Int. Ed.* **2006**, *45*, 7042–7046; d) V. Balzani, H. Bandmann, P. Ceroni, C. Giansante, U. Hahn, F.-G. Klamer, U. Müller, W. M. Müller, C. Verhaelen, V. Vicinelli, F. Vögtle, *J. Am. Chem. Soc.* **2006**, *128*, 637–648; e) M. D. Pluth, K. N. Raymond, *Chem. Soc. Rev.* **2007**, *36*, 161–171; f) C. A. Nijhuis, B. J. Ravoo, J. Huskens, D. N. Reinhoudt, *Coord. Chem. Rev.* **2007**, *251*, 1761–1780.
- [26] P. M. S. Monk, *The Viologens—Physicochemical Properties, Synthesis and Applications of the Salts of 4,4'-Bipyridine*, Wiley, Chichester, **1998**, p. 56 and 115.
- [27] H.-J. Kim, W. S. Jeon, Y. H. Ko, K. Kim, *Proc. Natl. Acad. Sci. USA* **2002**, *99*, 5007–5011.
- [28] V. Balzani, M. Clemente-León, A. Credi, B. Ferrer, M. Venturi, A. H. Flood, J. F. Stoddart, *Proc. Natl. Acad. Sci. USA* **2006**, *103*, 1178–1183.
- [29] a) J.-M. Lehn, *Prog. Polym. Sci.* **2005**, *30*, 814–831; b) K. Ohga, Y. Takashima, H. Takahashi, Y. Kawaguchi, H. Yamaguchi, A. Harada, *Macromolecules* **2005**, *38*, 5897–5904; c) C. A. Hunter, S. Tomas, *J. Am. Chem. Soc.* **2006**, *128*, 8975–8979; d) T. Park, S. C. Zimmerman, *J. Am. Chem. Soc.* **2006**, *128*, 14236–14237; e) K. A. Burke, S. Sivakova, B. M. McKenzie, P. T. Mather, S. J. Rowan, *J. Polym. Sci. Part A* **2006**, *44*, 5049–5059; f) H. Ohkawa, G. B. W. L. Lighthart, R. P. Sijbesma, E. W. Meijer, *Macromolecules* **2007**, *40*, 1453–1459; g) F. Huang, D. S. Nagvekar, H. W. Gibson, *Macromolecules* **2007**, *40*, 3561–3567; h) T. F. A. de Greef, E. W. Meijer, *Nature* **2008**, *453*, 171–173.
- [30] L. M. Tunstad, J. A. Tucker, E. Dalcanale, J. Weiser, J. A. Bryant, J. C. Sherman, R. C. Hegelson, C. B. Knobler, D. J. Cram, *J. Org. Chem.* **1989**, *54*, 1305–1312.
- [31] A. Credi, L. Prodi, *Spectrochim. Acta A* **1998**, *54*, 159–170.
- [32] R. A. Binstead, *SPECFIT*, Spectrum Software Associates, Chapel Hill, NC, **1996**.

Received: May 20, 2008  
Published online: August 12, 2008